

CHARACTERIZATION OF A COHESIVE SOIL BED USING A CONE PRESSUREMETER

Z. REHMANⁱ⁾, A. AKBARⁱⁱ⁾ and B. G. CLARKEⁱⁱⁱ⁾

ABSTRACT

A new cone pressuremeter has been developed at the University of Engineering and Technology, Lahore-Pakistan. The new device is called the Akbar Pressuremeter (APMT). This paper is based on the APMT testing of a cohesive soil deposit comprised of low plastic lean clay (CL) to sandy silty clay (CL-ML). The APMT testing, using a full-displacement technique, standard penetration tests and undisturbed samples, was carried out at two locations. The soil strength and type were determined using the undisturbed samples. The applied pressure-cavity strain curves of the APMT tests performed at different levels were analysed to determine soil strength and stiffness. The undrained shear strength of the undisturbed samples was determined in the laboratory by unconfined compression tests. This paper provides a comparison of the parameters interpreted from the pressuremeter and those determined from other field and laboratory methods.

Key words: clay, *in situ* horizontal stress, pressuremeter, shear modulus, shear strength, SPT (IGC: C8)

INTRODUCTION

Over the last half a century, a lot of research has been carried out around the world for the purpose of developing new *in situ* soil testing devices and data analysis procedures. These include cone penetrometers, pressuremeters, dilatometers etc. The devices have been developed to produce better quality soil parameters. However, many of these devices are sophisticated, and hence, expensive to buy or rent, making their use unaffordable for small projects.

The first full-displacement pressuremeter (FDPM) was developed by Withers et al. (1986). It is headed by a 15 cm² solid cone, which is pushed into place by displacing the ground. It measures the inflation pressure and the circumferential strain at three locations, 120° apart, at the centre of the membrane. The membrane is secured by a Chinese lantern, thus making the probe sophisticated. The latest Fugro cone pressuremeter has been further simplified by the use of a volume change measurement system, rather than strain gauges, to measure the expansion of the pressuremeter membrane. The assembly and test control have also been made easier (Zuidberg and Post, 1995), although the basic design has remained unchanged. While many efforts have been made to make it even simpler, no efforts had been made to measure the expansion of the pressuremeter membrane with a single transducer until 2001. Using a single transducer, Akbar (2001) developed the Newcastle full-displacement pres-

suremeter (NFDPM) keeping the length of the test section at 420 mm (Akbar et al., 2003), which is nearly the same as that of the FDPM developed by Withers et al. (1986).

A new version of the NFDPM pressuremeter has been developed at the Civil Engineering Department, University of Engineering and Technology, Lahore-Pakistan, which has a test section with a reduced length. It is called an Akbar Pressuremeter (APMT). It is also instrumented with a single transducer to measure the expansion of the membrane. During the SPT testing, the blows are recorded for the 305-mm penetration of the split spoon sampler, and therefore, the length of the pressuremeter probe's test section has also been kept at 305 mm in order to correlate the pressuremeter data with the SPT blows. The purpose of maintaining this similarity is to benefit from the long history of experience available on the SPT.

A testing programme comprised of field and laboratory tests was planned to check and/or improve the correlations among the APMT indices, the soil properties and the geotechnical design parameters by performing tests on an artificially prepared cohesive soil bed. This paper presents a comparison of the various soil properties determined from the pressuremeter with those from the SPT and laboratory tests.

AKBAR PRESSUREMETER (APMT)

A full-displacement pressuremeter has been developed using mostly local resources by making some modifica-

ⁱ⁾ Ph.D. Student, Civil Engineering Department, University of Engineering and Technology, Lahore-Pakistan (gzia718@hotmail.com).

ⁱⁱ⁾ Professor, ditto (azizakbar59@hotmail.com).

ⁱⁱⁱ⁾ Professor, School of Civil Engineering, University of Leeds, UK (b.g.Clarke@leeds.ac.uk).

The manuscript for this paper was received for review on June 4, 2009; approved on May 12, 2011.

Written discussions on this paper should be submitted before May 1, 2012 to the Japanese Geotechnical Society, 4-38-2, Sengoku, Bunkyo-ku, Tokyo 112-0011, Japan. Upon request the closing date may be extended one month.

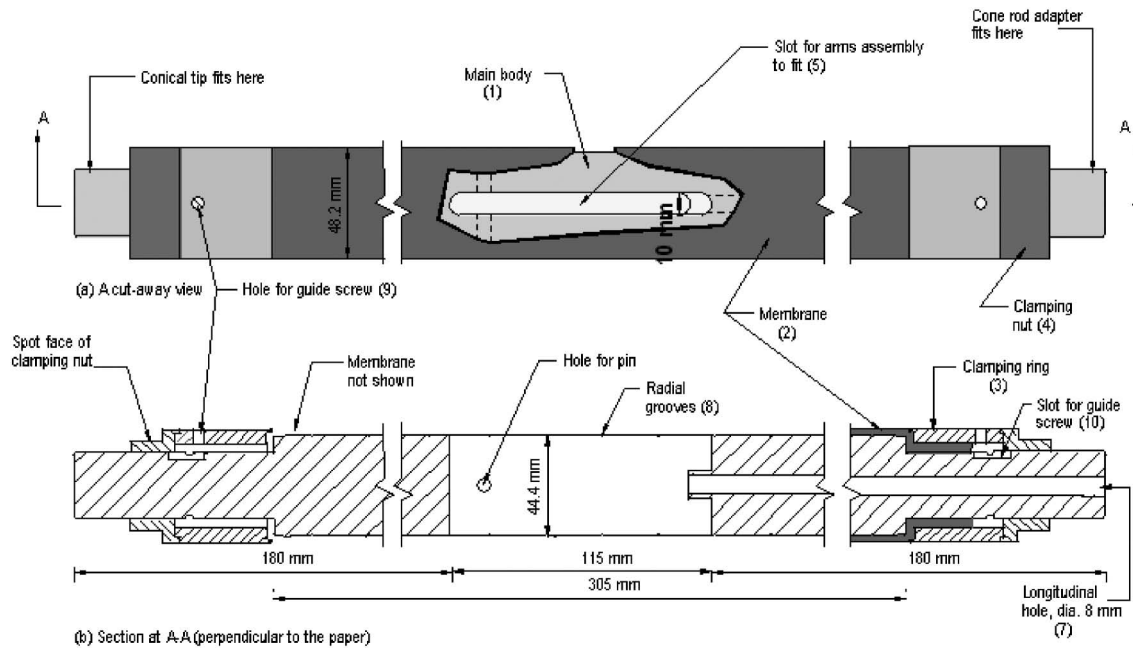


Fig. 1. Akbar pressuremeter (APMT) probe

tions to the design for the NFDPM developed by Akbar (2001). The new device is called the Akbar Pressuremeter (APMT). The main body of the probe of the APMT is made of high-strength stainless steel. Figure 1 presents a view of the probe and the cross section of the main body along with some accessories. The test section (L) is 44.4 mm in diameter and 305 mm in length. With the membrane in place, the outer diameter of the probe (D) is 48.2 mm. Therefore, the L/D ratio is 6.3. Both ends of the main body are identical. One end is connected to a pressure hose and an electrical cable by a re-usable hydraulic fitting. A 45° stainless steel cone, with a maximum diameter of 50.8 mm (surface area of 28.5 cm²), is screwed onto the other end. Thus, the cone creates a cavity with a diameter about 5% greater than that of the probe. The oversized cavity helps in two ways during the probe installation in the ground. The first way is that the dragging force on the membrane, due to friction with the soil, is reduced. This prevents the ends of the membrane from being pulled out of the clamping ring. The second way is that it can also be pushed safely through a soil that contains gravel. This eliminates the use of the Chinese lantern, thus making its assembly simpler and more cost-effective.

The main body (Fig. 1(a)) is 115 mm in length and has a slot in the middle, 10 mm in width, for the assembly of the expansion arms (Fig. 2). A longitudinal hole, 8 mm in diameter, is drilled from one end (the end to which the hydraulic coupling is connected) up to the central slot. This hole houses the transducer wires and transmits pressurised gas, which inflates the membrane. The radial grooves have been machined to enable dry nitrogen gas (N_2) pressure to simultaneously reach everywhere underneath the membrane. This allows the whole length of the membrane to expand equally under uniform soil condi-

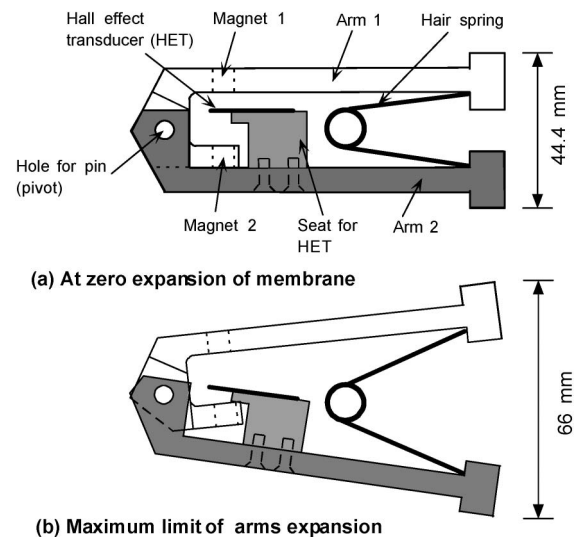


Fig. 2. Expansion arms

tions around the probe.

The expansion arms, made from stainless steel, move outwardly about a pivot point. This outward movement is activated by a hair spring. At zero expansion of the membrane, the distance between the outer surfaces of the arms is the same as that of the main body (i.e., 44.4 mm), as shown in Fig. 2(a). The arms can move apart radially from 44.4 mm to a maximum of 66 mm. This limit is reached when a part of arm-1, containing magnet 2, comes in contact with the projecting part of the seat for the linear output Hall Effect Transducer (HET), as shown in Fig. 2(b). According to this design, the expansion of the arms is about 45% of the diameter of the probe. The HET has been mounted on the seat with glue, positioning it between the two magnets located in arm-1. The expan-

sion of the arms changes the output of the HET mounted inside the arms, as shown in Fig. 3. The HET is connected to the analog and the digital (A/D) data-logger at the surface using an electrical cable, which passes through the pressure hose. One end of the pressure hose is permanently fixed to the pressuremeter probe, while the other end is fixed to the gas-electric separator during the *in situ* testing. The gas-electric separator separates the cable and the hose, while the pressure transducer fitted to the separator measures the gas pressure applied during the membrane expansion.

The pressuremeter membrane consists of two layers. The inner layer, 2.20 mm in thickness, is made from Nitrile. It is reinforced by encasing with a Nylon cover, 1.10 mm inn thickness. The inside and outside diameters of the rubber membrane are 31.75 and 38.35 mm, respectively.

CALIBRATION FOR SYSTEM STIFFNESS

Before calibration of the system stiffness, the HET and the pressure transducer were calibrated. Calibration of the HET has been described earlier and is shown in Fig. 3. Calibration of the pressure transducer was carried out using a Budenberg dead weight gauge. The calibration data for the pressure transducer is plotted in Fig. 4. After assembling the whole system (Fig. 5), the calibration of the membrane stiffness was carried out by increasing the gas pressure in small increments of about 10 kPa, maintaining each increment for 60 seconds. In 60 seconds, the radial expansion of the membrane was found to be almost complete. The same duration was used for the Ménard pressuremeter tests. When the arms had moved out to their maximum design distance, which was reflect-

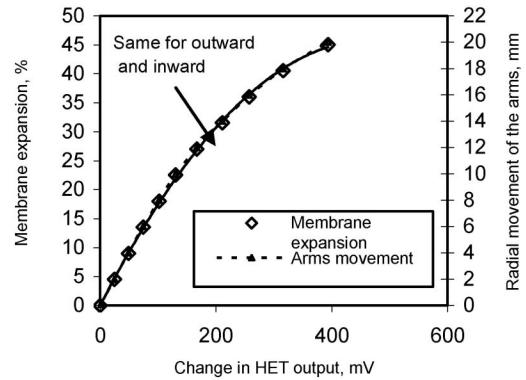


Fig. 3. Typical calibration data plot for HET in APMT

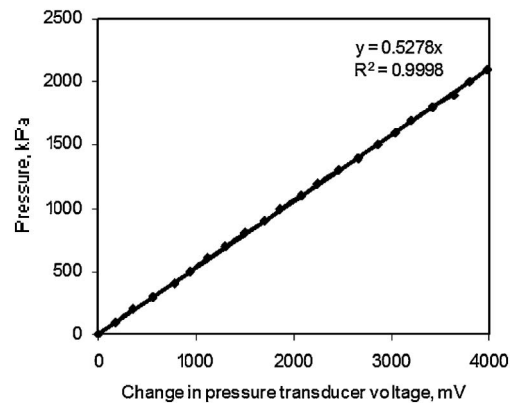


Fig. 4. Typical calibration data plot for pressure transducer

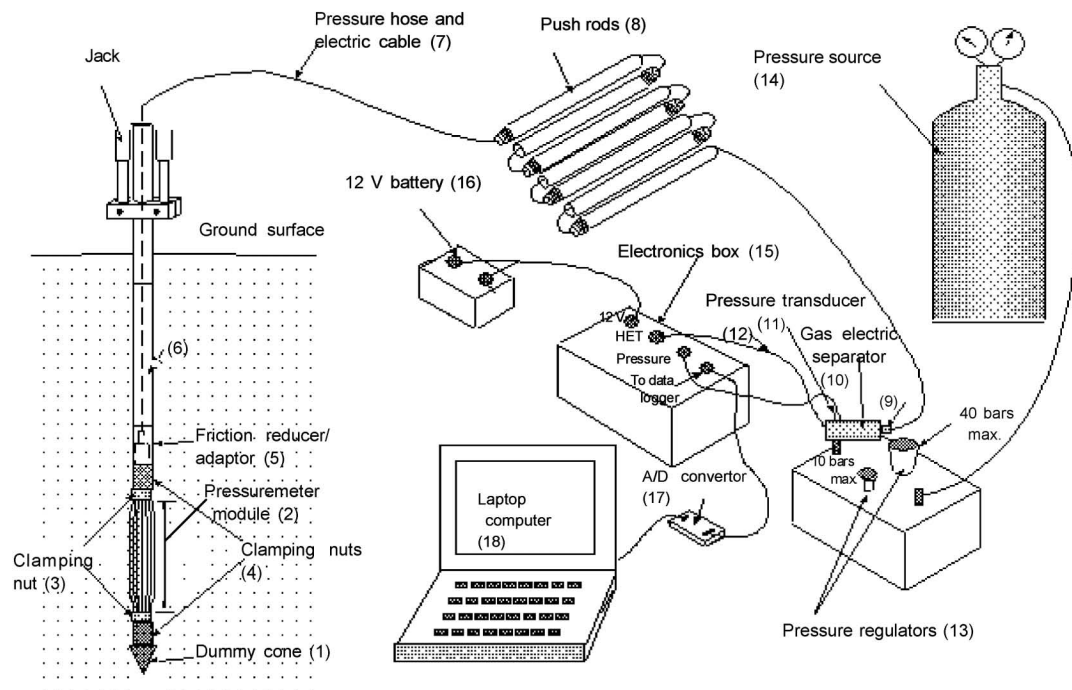


Fig. 5. On-site assembly of APMT equipment

ed by the constant output of the HET, unloading was commenced using similar decrements until the full contraction of the arms. The radial expansion of the membrane is plotted in percentage against the applied gas pressure in Fig. 6.

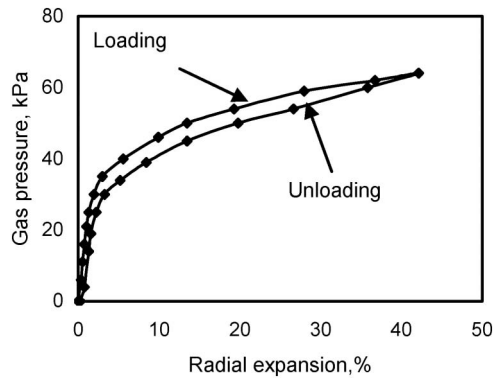


Fig. 6. Typical calibration data plot for radial expansion of APMT membrane

TEST SITE

The APMT tests were carried out at an Open Area of the Civil Engineering Department, University of Engineering and Technology, Lahore-Pakistan. For this purpose, a test pit, 3 m × 3 m and 5 m in depth, was excavated and backfilled with borrowed cohesive soil consisting of low plastic lean clay (CL) to sandy silty clay (CL-ML). At the time of the backfilling, this soil had a low moisture content (less than the plastic limit) and was in a disintegrated form. The groundwater table was much lower than 5.0 m. During the backfilling, the pit was kept filled with water and the borrowed material was dropped manually from the surface into the pit. This technique was employed to obtain a uniform moisture content and density conditions in the test pit. This methodology of soak filling also simulates the process through which natural deposits are usually formed. The APMT tests were conducted after a lapse of about one year to allow the soil to achieve conditions of equilibrium in terms of uniformity in moisture content and degree of saturation. This was indicated by a comparison of the natural moisture content and the liquid limit values of the soil samples given in Table 1. The moisture content, which

Table 1. Summary of Classification tests, SPT and unconfined compression tests

Location: Open area, Civil Engineering Department, University of Engineering & Technology, Lahore

Sampling	Depth (m)	LL (%)	PL (%)	PI	Gravel (%)	Sand (%)	Silt/clay (%)	SPT N value	Soil type	NMC (%)	Liquidity Index	γ_b (kN/m ³)	c_u (kPa)
1	2	3		4	5	6	7	8	9	10		11	12
SPT1	1	25		5	0	30	70	2	CL-ML	—		—	—
	2	27		5	0	17	83	3	CL-ML	—		—	—
	3	28		5	0	20	80	2	ML	—		—	—
	4	27		5	0	10	90	4	CL-ML	—		—	—
	5	28		8	0	5	95	6	CL-ML	—		—	—
SPT2	1	27		7	0	13	87	2	CL-ML	—		—	—
	2	28		7	0	12	88	3	CL-ML	—		—	—
	3	28		5	0	9	91	2	CL-ML	—		—	—
	4	27		7	1	8	91	3	CL-ML	—		—	—
	5	29		5	4	5	91	6	ML	—		—	—
UDS1	1	22	15	7	0	32	68	—	CL-ML	13.6	−0.20	19	29
	2	28	19	9	0	17	83	—	CL	20.1	0.12	19.2	44
	3	26	19	7	0	19	81	—	CL-ML	22.4	0.49	18.8	38
	4	32	21	11	0	1	99	—	CL	25.9	0.45	20.1	45
	5	28	20	8	26	12	62	—	CL	21.7	0.21	20.8	48
UDS2	1	29	19	10	0	12	88	—	CL	18.2	−0.08	19.6	30
	2	26	17	9	0	21	79	—	CL	33.8	1.87	18.8	35
	3	28	20	8	0	20	80	—	CL	20.8	0.10	19.9	32
	4	27	20	7	5	5	90	—	CL-ML	20.7	0.10	20.6	32
	5	31	23	8	0	5	95	—	CL	22.5	−0.06	20.1	51

was more than the liquid limit values at the time of the backfilling, decreased and was found to generally be between the liquid and the plastic limit yielding liquidity index values, namely, between 0 and 1, indicating soil in the plastic state.

FIELD TESTING

The equipment was assembled at the site, as shown in

the schematic sketch in Fig. 5. The APMT testing was carried out at two locations (APMT-1 and APMT-2), as shown in Fig. 7. Figure 8 shows the pushing arrangement used for the full-displacement pressuremeter tests using a reaction frame anchored in the ground at four locations. The probe was pushed into the ground using a jack and push rods. The pushing of the APMT was halted when the centre of the test section reached the desired test depth and was then resumed as soon as the APMT probe was

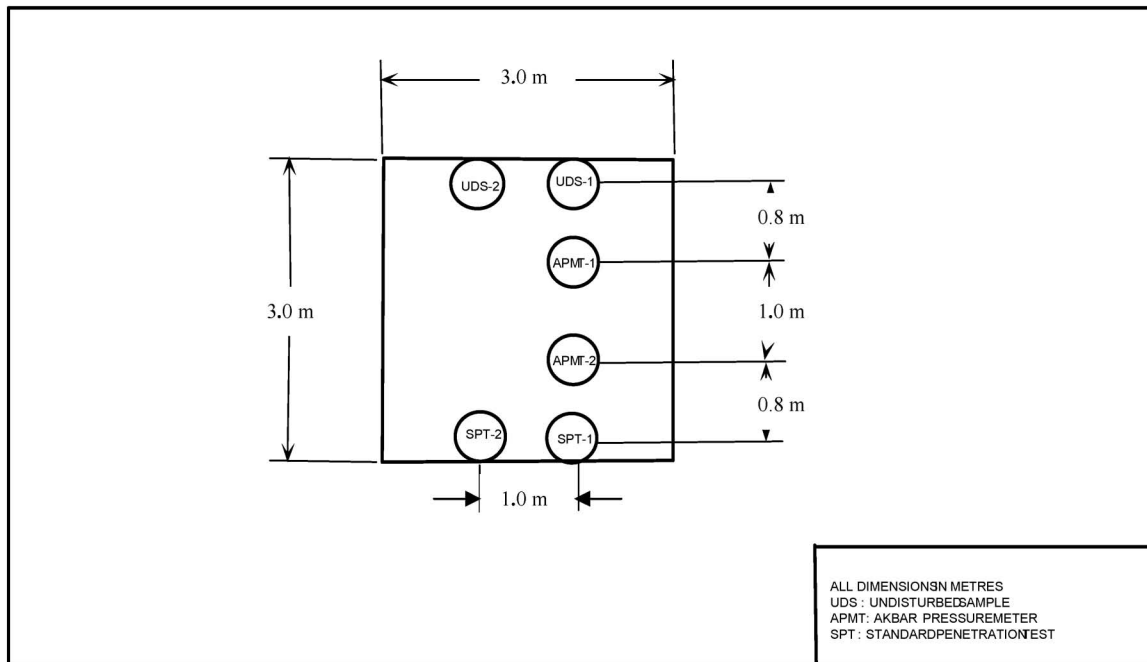


Fig. 7. Field testing plan

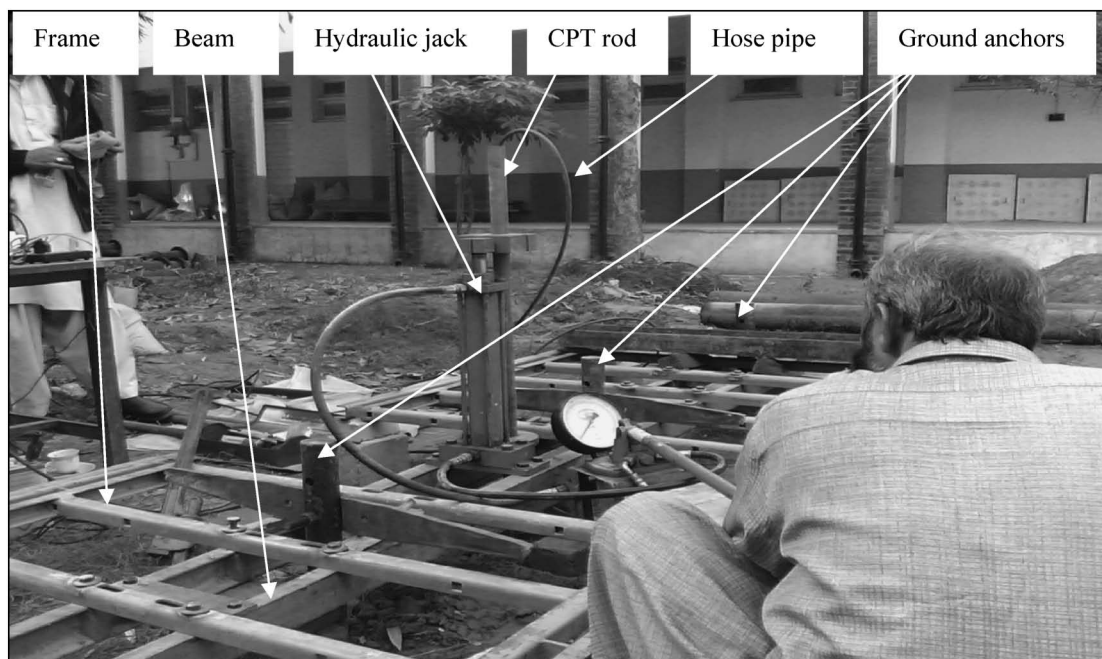


Fig. 8. Pushing arrangement

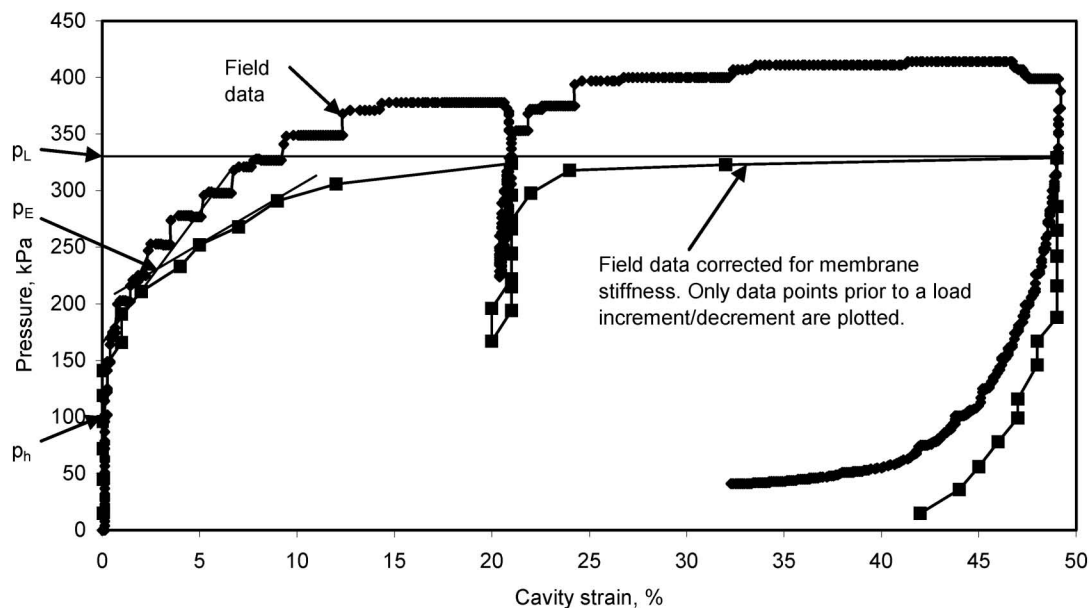


Fig. 9. Typical applied pressure-cavity strain curve at depth of 2.0 m

deflated after each test. The testing interval was kept at 1 m, so that each test would not be affected by the previous one. Stress-increment controlled tests were carried out, which is a common procedure when testing with a self-boring pressuremeter, a full-displacement pressuremeter (Clarke, 1996) or a Ménard pressuremeter. Pressure was applied in increments of about 25 kPa and maintained for 60 seconds with data recorded every 1 second. The unloading was conducted from an expansion of about 45% of the initial cavity size, as the arms could not move beyond this cavity strain. An unload-reload cycle was also included in each test during the loading in order to estimate the elastic shear modulus. Figure 9 shows a typical applied pressure-cavity strain curve at a depth of 2.0 m.

The SPT and the undisturbed sampling were carried out at nearby locations according to the planned levels of APMT testing shown in Fig. 7. The recorded SPT blows are presented in Table 1. The SPT N values range from 2 to 6, indicating very soft to medium stiff clays (Bowles, 1996). Undisturbed samples (UDS) were obtained using Shelby tubes with a diameter of 38 mm. This technique of soil sampling, although commonly used, does disturb the soil sample to some extent. Hence, the term 'relatively undisturbed' seems appropriate. The UDS were retrieved from two boreholes, at the same depths as the APMT tests, close to the APMT test locations. The boreholes were advanced through auguring. In addition, Shelby tubes were gently hammered into the soil to obtain relatively undisturbed soil samples.

LABORATORY TESTING

The following tests were performed on undisturbed and disturbed soil samples to determine the soil strength and type:

- Unconfined Compression Test (ASTM D2166)

- Grain Size Analysis (ASTM D422)
- Liquid Limit (LL) Test (ASTM D4318)
- Plastic Limit (PL) Test (ASTM D4318)

Table 1 presents a summary of the laboratory test results. Based on a sieve analysis, the percentages of gravel, sand and silt and/or clay in the different samples were between 0 and 26%, 1 and 32% and 62 and 99%, respectively. The liquid limit values of the soil samples ranged from 22 to 32% and the plasticity index values ranged from 5 to 11. On the basis of these classification tests, the soils can be said to consist of low plastic lean clay (CL) to sandy silty clay (CL-ML). The natural moisture content (NMC) values ranged from 13.6 to 33.8% and the bulk unit weight (γ_b) values ranged from 18.8 to 20.8 kN/m³. The undrained shear strength (c_u) values determined through unconfined compression tests varied from 29 to 51 kPa.

ANALYSIS OF PRESSUREMETER DATA

Figure 9 shows plots for the uncorrected as well as the corrected applied pressure and cavity strain data for the membrane stiffness for tests at a depth of 2.0 m. The corrected curve shows only the data points prior to the load increment and/or decrement.

The limit pressure (p_L) is defined as the pressure required to double the initial volume of the cavity. Since the HET can record the strain of the cavity expansion only up to about 45%, the limit pressures have been determined by extrapolation to the maximum pressure to be reached in a PMT test at which the cavity will continue to expand indefinitely (Clarke, 1995), as shown in Fig. 9. Two other pressures, p_F and p_h , are also shown in Fig. 9. p_F is the yield pressure in the APMT test curve; it is obtained from the point of intersection of the tangents drawn on the initial elastic portion and the initial portion of the plastic

yielding of the APMT curve, as shown in Fig. 9. p_h is the pressure at the start of the elastic yielding in the APMT test curve; it is the maximum pressure corresponding to the zero percent cavity strain in the APMT test curve, as shown in Fig. 9.

UNDRAINED SHEAR STRENGTH (c_u)

For the full-displacement technique, the undrained shear strength (c_u) has been determined from the unloading part of the APMT curve using the procedure proposed by Houlsby and Withers (1988). According to the procedure, the cavity expansion pressures are plotted against $\{-\ln [(m+1)/2] (\epsilon_m - \epsilon)\}$ values for the final unloading part of the curve. The value for m is taken as 1 for the cylindrical expansion and as 2 for the spherical expansion, ϵ is the cavity strain at any pressure and ϵ_m is the

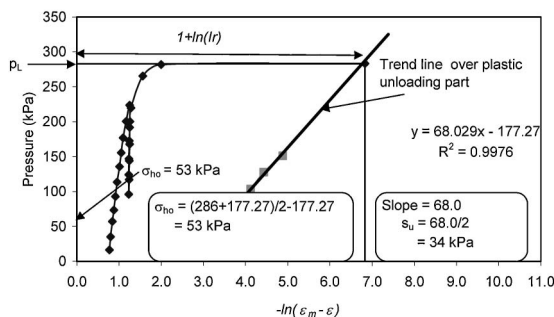


Fig. 10. Analysis of APMT data at depth of 1.0 m in soft clay according to Houlsby and Withers (1988)

maximum strain reached in that test. σ_{ho} is determined by identifying the mid-point between the limit pressure (p_L) and the intercept of the trend line over the plastic unloading part. For the APMT, m is taken as 1. The slope of the line is $2c_u(2+m)/3$, which reduces to $2c_u$ for APMT. The abscissa of the intersection of the limit pressure and the plastic unloading line is $1 + \ln(I_r)$, where I_r is the rigidity index ($= G/s_u$). With known values of $1 + \ln(I_r)$ and s_u , G can be determined. This procedure is graphically explained in Fig. 10. This figure presents a plot of the expansion pressure against $[-\ln (\epsilon_m - \epsilon)]$. The undrained strength (c_u) values determined according to this procedure are shown in column 8 of the summary in Table 2. The c_u values for the location of APMT-1 lie between 19 and 46 kPa and according to BS 8004:1986, the clay can be classified as being in a soft to firm state. At the APMT-2 location, the c_u values vary from 25 to 42 kPa, which indicates firm clay. A comparison of the shear strength values at the same level from both locations shows that the difference in c_u values varies from 1 to 21 kPa. As already discussed, soils in the bed consist of silty clay, lean clay or silt and the soils and their moisture contents are not the same at certain test levels (Table 1). This is to be expected, due to the process by which this bed has been prepared. Hence, the consistency limits of the soil bed vary both laterally and vertically.

Figure 11 presents a comparison of the undrained shear strength (c_u) values determined from the pressuremeter and unconfined compression tests (UCT). For this comparison, locations APMT-1 and APMT-2 correspond to locations UDS-1 and UDS-2, respectively. The c_u values from these two sources show a good agree-

Table 2. Summary of APMT test results

Location	Depth (m)	p_h (kPa)	p_F (kPa)	p_L (kPa)	$p_L - p_F$ (kPa)	Houlsby et al. (1988)		Strain range			Unload-reload cycle Average stiffness		Houlsby and Withers (1988)		
								ϵ_{max} and ($\epsilon_{max} - 0.2\%$)		ϵ_{min} and ($\epsilon_{min} + 0.2\%$)					
								First unloading	Final unloading	Reloading					
						σ_{ho} (kPa)	c_u (kPa)	G_{u1} (MPa)	G_{u2} (MPa)	G_r (MPa)	Cycle slope (MPa)	G_{ur} (MPa)	$1 + \ln(I_r)$	I_r	G (MPa)
1	2	3	4	5	6	7	8	9	10	11	12	13	14	15	16
APMT-1	1	25	150	283	133	53	34	7.3	5.5	6.4	13.1	6.6	6.77	321	10.9
	2	100	225	329	104	76	36	8.3	6.6	6.1	13.6	6.8	7.02	412	14.8
	3	70	145	190	45	58	19	2.4	3.5	2.9	4.6	2.3	6.99	399	7.5
	4	41	260	388	128	76	46	6.9	10.6	6.9	17.7	8.9	6.86	351	16.0
	5	50	225	375	150	72	43	9.2	8.7	10.7	18.9	9.5	6.97	392	17.0
APMT-2	1	40	180	268	88	55	31	6.3	5.7	7.4	10.5	5.3	6.87	354	11.0
	2	80	170	237	67	43	29	5.1	3.5	7.4	8.7	4.4	6.76	317	9.2
	3	100	225	328	103	82	35	6.5	5.7	6.6	12.3	6.2	7.01	407	14.3
	4	50	125	232	107	57	25	3.6	5.9	4.5	5.7	2.9	6.88	358	8.9
	5	45	235	362	127	70	42	9.2	8.7	10.7	18.9	9.5	6.87	354	14.9

G_{ur} = Col.12/2

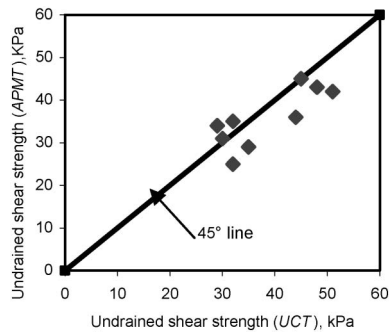


Fig. 11. Comparison of undrained shear strength values from APMT and laboratory tests

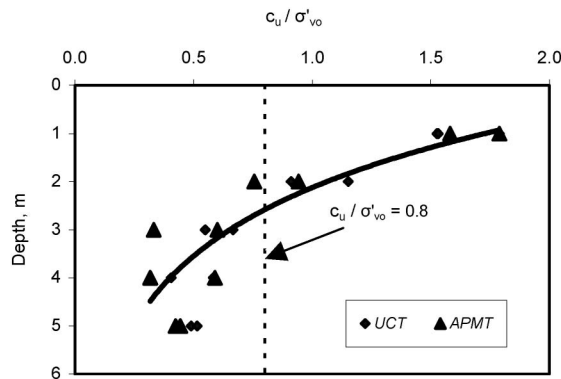


Fig. 12. Profiles of c_u/σ'_{v0} vs depth

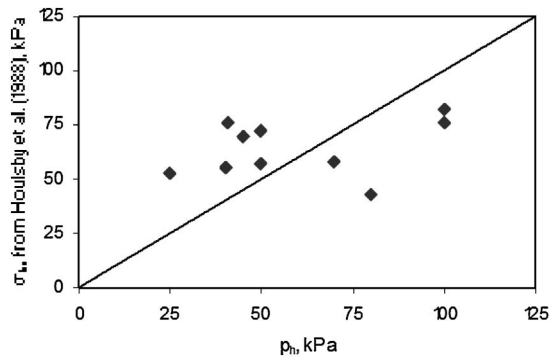


Fig. 13. Comparison of σ_{ho} from Housby and Withers's method (1988) with pressure p_h

ment.

Figure 12 shows a plot for c_u/σ'_{v0} against depth. The c_u/σ'_{v0} values, in general, decrease with depth. Except for six data points for soft to firm clay, which show c_u/σ'_{v0} ratios greater than 0.8, probably due to the desiccation effects near the surface, all other ratios are less than 0.8. According to Lunne et al. (1992), the subsoil with $c_u/\sigma'_{v0} \leq 0.8$ is comprised of young clay. The soil bed tested is one year old. Since the groundwater table during this time is much deeper than 5 m, the excess water from the poured soil seeped into the surrounding natural soil. Near the surface, however, the reduction in water content was due to drying by the sun and air and resulted in c_u/σ'_{v0} ra-

tios greater than 0.8.

IN SITU HORIZONTAL STRESS (σ_{ho})

The *in situ* horizontal stress, σ_{ho} , has been estimated using the procedure suggested by Housby and Withers (1988), which according to them is not reliable. A sample calculation is shown in Fig. 10. In column 7 of Table 2, σ_{ho} values are presented which range from 53 to 76 kPa for APMT-1 and 43 to 82 kPa for APMT-2. Out of ten data points in Fig. 13, only four points show p_h values higher than σ_{ho} , which is logical due to the fact that the soil is displaced laterally during the installation of the APMT probe into the soil. The six data points which show an illogical trend could be the reason for the low reliability of this method, as stated by Housby and Withers (1988). A similar trend has been reported by Akbar (2001).

SHEAR MODULUS (G)

The shear modulus (G) was determined in a number of ways from the pressuremeter stress-strain curve, as listed below:

- Secant unload modulus (G_{u1}) from the first unloading part measured over a strain range of 0.2%
 G_{u1} values are presented in column 9 of Table 2.
- Secant unload modulus (G_{u2}) from the final unloading part
 G_{u2} values are presented in column 10 of Table 2.
- Secant reload modulus (G_r) from the reloading part measured over a strain range of 0.2%
 G_r values are presented in column 11 of Table 2.
- Secant modulus (G_{ur}) from the unload-reload cycle
 G_{ur} values are presented in column 13 of Table 2.
- Modulus (G) by the Housby and Withers (1988) method

G values are presented in column 16 of Table 2.

The profiles of the shear moduli determined from different methods are shown in Fig. 14. As expected, the data are scattered because the shear moduli have been obtained at different stress and strain levels. The shear modulus values determined by the Housby and Withers (1988) method are higher as compared to those determined by other methods.

If Poisson's ratio ν is known, modulus of elasticity E can then be determined using the following relation:

$$E = 2(1 + \nu)G \quad (1)$$

Figure 15 shows the variation in the elemental secant shear modulus (final unloading) normalised with respect to the horizontal effective stress against the current cavity strain (elemental) for the APMT data. The effective horizontal stress is taken as the effective applied pressure at the start of unloading since this represents the maximum pressure to which the soil is loaded prior to unloading. In Fig. 15, current cavity strain ϵ_{curr} is defined as

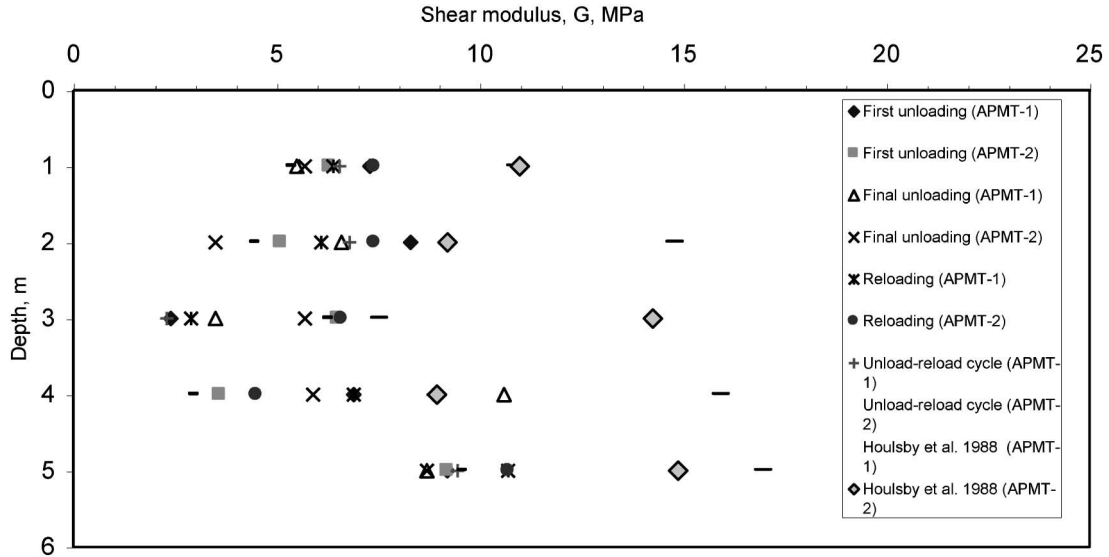


Fig. 14. Shear moduli profiles

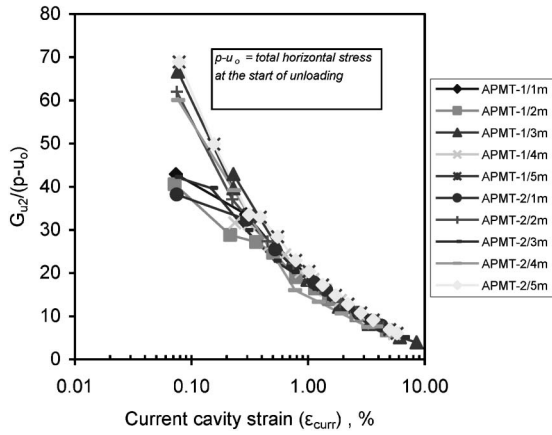


Fig. 15. Variation in elemental shear modulus with strain

$$\varepsilon_{curr} = \left(\frac{\varepsilon_s - \varepsilon_m}{1 + \varepsilon_m} \right) \quad (2)$$

where ε_s is the elemental cavity strain at any point of the cycle and ε_m is the maximum cavity strain during unloading for G_u .

The results in Fig. 15 show that the stiffness responses present more scatter at small levels of strain, namely, below about 0.2%. The scatter is reduced with strain. The early scatter may be due to the consolidation which takes place at the start of unloading and/or to the limitation of the measurements. The large scatter in the small strain secant modulus values has also been explained by Muir Wood (1990). According to him, it is difficult to identify precisely the start of an unloading or reloading phase; therefore, these effects may tend to obscure the small strain behaviour of the soil.

Figure 16 shows a plot of the strain amplitude against the cycle shear modulus (G_{ur}) normalised by the applied effective pressure, ($p-u_o$) at the start of unloading. The

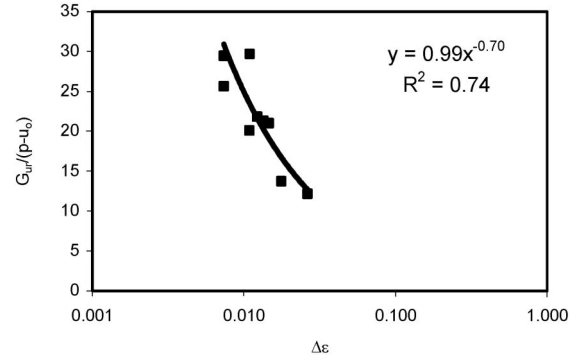


Fig. 16. Normalised shear modulus plotted against strain amplitude

plot shows that the normalised moduli are a function of the strain amplitude, as expected, with a slightly lower normalised modulus at a higher strain amplitude. Houslsby and Nutt (1993) reported similar observations for the unload-reload shear modulus.

CORRELATIONS BETWEEN DIFFERENT PARAMETERS

Using the available data, correlations between different parameters have been developed by employing linear regression analyses. The developed correlations along with possible comments are presented below:

- PMT shear modulus vs. SPT N values

The shear modulus values obtained based on the unloading (G_{ul}) and the reloading (G_r) parts of the unload-reload cycle and the N values for the same depth have been plotted in Fig. 17. However, the variation in shear modulus with the N values can be represented by the following equation:

$$G = 3.61 \ln N + 2.73 \quad (3)$$

where G is in MPa.

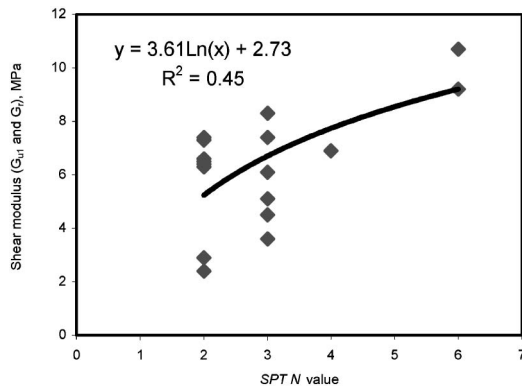


Fig. 17. Correlation between shear modulus and SPT N value

For most clay soils, $\nu = 0.4\text{--}0.5$ (Bowles, 1996). Taking $\nu = 0.45$, Eq. (2) yields $E = 29 G$. By substituting the proposed equation for the shear modulus, given by Eq. (3), this relation is reduced to the following equation:

$$E = 10.5 \ln N + 7.9 \quad (4)$$

where E is in MPa.

For the given values of N , the value of E ranges from 15.2 to 26.7 MPa (using Eq. (4)) for soft to firm clay. Bowles (1996) suggested a range of 5 to 50 MPa for soft to medium hard clays. Therefore, Eq. (3) can be used to estimate the shear modulus of soft to firm clays.

• Undrained shear strength vs. SPT N values

Figure 18 shows the plots of the N values against the undrained shear strength determined from the APMT data for very soft to medium stiff clays. Although there is scatter in the data, the general trend is an increase in strength with an increase in N . A regression analysis yields the following equation:

$$c_u = 9.18 N \quad (5)$$

where c_u is in kPa.

Terzaghi and Peck (1967), Parcher and Means (1968) and Tschebotarioff (1973) developed the relations between these parameters, including soil consistency, given by Eqs. (6), (7) and (8), respectively, as

$$c_u = 664 N \text{ (Very soft to very stiff clays)} \quad (6)$$

where c_u is in kPa.

$$c_u = 6.64 N \text{ (Very soft to very stiff clays)} \quad (7)$$

where c_u is in kPa.

$$c_u = 7.86 N \text{ (Very soft to stiff clays)} \quad (8)$$

where c_u is in kPa.

Among Eqs. (6) to (8), the proposed Eq. (5) is closest to Eq. (8).

• Limit pressure vs. SPT N values

In Fig. 19, the limit pressure (p_L) values have been plotted against the N values, corrected only for the effective overburden pressure (Bowles, 1996). In general, an increasing trend for p_L with N can be seen from the figure. The proposed correlation is presented below.

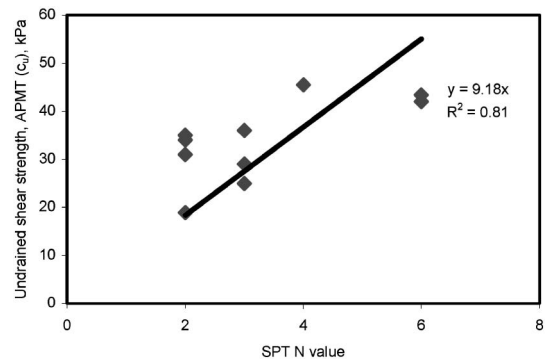


Fig. 18. Correlation between undrained shear strength and SPT N value

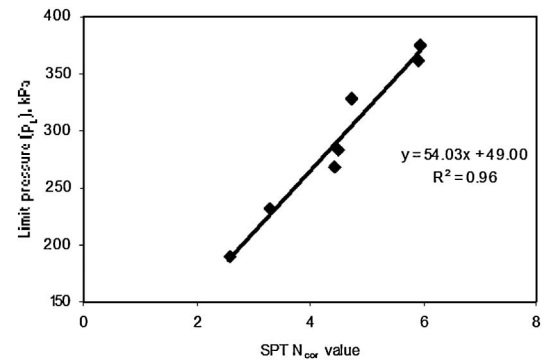


Fig. 19. Correlation between limit pressure and SPT N value

$$p_L = 54.03 N_{cor} + 49.00 \quad (9)$$

where p_L is in kPa.

Yagiz et al. (2008) developed the following correlation between the same parameters:

$$p_L = 29.45 N_{cor} + 219.7$$

(Medium to very stiff sandy silty clay) (10)

where p_L is in kPa.

The trend seen in Eqs. (9) and (10) is similar and the difference in the slope may be due to the difference in soil types.

CONCLUSIONS

A new cone pressuremeter has been developed using most of the local resources. It has been tested successfully using cohesive soils varying in consistency from soft to firm. On the basis of the analyses of the pressuremeter data and the discussions on the results, the following conclusions can be drawn:

- The data obtained from the new device can be analysed using the available cavity expansion theory.
- The undrained shear strength derived from the APMT data analyses compares well with that determined from unconfined compression tests in the laboratory.
- The proposed correlations for soft to firm clays are

presented as

S.No.	Proposed correlation
1	$G = 3.61 \ln N + 2.73$, where G is in MPa.
2	$c_u = 9.18 N$, where c_u is in kPa.
3	$p_L = 54.03 N_{cor} + 49.00$, where p_L is in kPa.

The correlations developed in this study are thought to be in good agreement with those of previous similar studies, although such studies are site-specific and are not universal due to the varying nature of soil. It should also be noted that soils at testing and sampling locations cannot be identical. This factor may result in the scatter of data.

REFERENCES

- 1) Akbar, A. (2001): Development of low cost in-situ testing devices, *Ph.D. Thesis*, Department of Civil Engineering, University of Newcastle, Newcastle Upon Tyne, UK.
- 2) Akbar, A., Clarke, B. G. and Allen, P. G. (2003): A low cost newcastle full-displacement cone pressuremeter, *UET Research Journal*, **14**, Jan. 2003, Nos. 1-2, 21-25, Lahore.
- 3) Bowles, J. E. (1996): *Foundation Analysis and Design*, 5th Edition, McGraw Hill Book Company, New York.
- 4) Clarke, B. G. (1995): *Pressuremeters in Geotechnical Design*, Blackie Academic and Professional, London.
- 5) Clarke, B. G. (1996): Pressuremeter testing in ground investigation, Part I-site operations, *Proc. Instn. Civ. Engr. Geotech. Engng.*, **119**, April, 96-108.
- 6) Houlsby, G. T. and Withers, N. J. (1988): Analysis of the cone pressuremeter test in clay, *Geotechnique*, **38**(4), 575-587.
- 7) Houlsby, G. T. and Nutt, N. R. F. (1993): Development of the cone pressuremeter, *Predictive Soil Mechanics, Proc. Wroth Memorial Symp.*, Oxford, 254-271.
- 8) Lunne, T., Lacasse, S. and Rad, N. S. (1992): General report: SPT, CPT, pressuremeter testing and recent developments in in-situ testing, *Proceedings, 12th International Conference on Soil Mechanics and Foundation Engineering*, **4**, Rio de Janeiro, 2339-2403.
- 9) Muir-Wood, D. (1990): Strain dependent moduli and pressuremeter tests, *Geotechnique*, **40**(26), 509-512.
- 10) Parcher, J. V. and Means, R. E. (1968): *Soil Mechanics and Foundations*, Charles E. Merrill, Columbus, Ohio.
- 11) Terzaghi, K. and Peck, R. B. (1967): *Soil Mechanics in Engineering Practice*, John Wiley, New York, 729.
- 12) Tschebotarioff, G. P. (1973): *Foundations, Retaining, and Earth Structures*, 2nd edition, McGraw-Hill, New York.
- 13) Withers, N. J., Schaap, L. H. J. and Dalton, C. P. (1986): The development of a full displacement pressuremeter, *The Pressuremeter and Its Marine Applications: Second International Symposium*, ASTM STP 950, 38-56.
- 14) Yagiz, S., Akyol, E. and Sen, G. (2008): Relationship between the standard penetration test and the pressuremeter test on sandy silty clays: a case study from Denizli, *Bull. Eng. Geol. Environ.*, **67**, 405-410.
- 15) Zuidberg, H. M. and Post, M. L. (1995): The cone pressuremeter: An efficient way of pressuremeter testing, *Proc. 4th Int. Symp. on Pressuremeter Testing (ISP4), The Pressuremeter and its New Avenue*, Balkema, 387-394.